pH Dependent Competition between Y_Z and Y_D in Photosystem II Probed by Illumination at 5 K†

Kajsa G. V. Havelius and Stenbjörn Styring*

Molecular Biomimetics, Department of Photochemistry and Molecular Science, Uppsala University, Ångström Laboratory, P.O. Box 523, S-751 20 Uppsala, Sweden

Received February 23, 2007; Revised Manuscript Received April 27, 2007

ABSTRACT: The photosystem II (PSII) reaction center contains two redox active tyrosines, Y_Z and Y_D, situated on the D1 and D2 proteins, respectively. By illumination at 5 K, oxidation of Y_Z in oxygen-evolving PSII can be observed as induction of the Split S_1 EPR signal from $Y_Z^\bullet$ in magnetic interaction with the $CaMn_4$ cluster, whereas oxidation of Y_D can be observed as the formation of the free radical EPR signal from $Y_D^\bullet$. We have followed the light induced induction at 5 K of the Split S_1 signal between pH 4−8.5. The formation of the signal, that is, the oxidation of Y_Z, is pH independent and efficient between pH 5.5 and 8.5. At low pH, the split signal formation decreases with pK_a ∼4.7−4.9. In samples with chemically pre-reduced Y_D, the pH dependent competition between Y_Z and Y_D was studied. Only Y_Z was oxidized below pH 7.2, but at pH above 7.2, the oxidation of Y_D became possible, and the formation of the Split S_1 signal diminished. The onset of Y_D oxidation occurred with pK_a ∼8.0, while the Split S_1 signal decreased with pK_a ∼7.9 demonstrating that the two tyrosines compete in this pH interval. The results reflect the formation and breaking of hydrogen bonds between Y_Z and D1-His190 (His_Z) and Y_D and D2-His190 (His_D), respectively. The oxidation of respective tyrosine at 5 K demands that the hydrogen bond is well-defined; otherwise, the low-temperature oxidation is not possible. The results are discussed in the framework of recent literature data and with respect to the different oxidation kinetics of Y_Z and Y_D.

Photosystem II (PSII)[1] in the thylakoid membrane of higher plants, algae, and cyanobacteria uses light energy to reduce plastoquinone with electrons from water (*2*, *3*). The D1 and D2 subunits form the reaction center dimer, which holds all of the redox active cofactors necessary for this catalytic process (*4*, *5*). After light is absorbed, charge separation between the primary donor P_{680} and the first electron acceptor pheophytin creates the charge pair $P_{680}^+Pheo^-$. The electron is further transferred to Q_A and subsequently to Q_B, which after two reductions and protonation separates from PSII into the thylakoid membrane. Under normal conditions, P_{680}^+ is reduced by an electron from the water-oxidizing $CaMn_4$ cluster (*6*, *7*) via the redox active tyrosine residue, Y_Z (*4*, *5*, *8*, *9*). During catalysis, the $CaMn_4$ cluster cycles through a series of intermediate states denoted the S_n-states ($n = 0-4$) to remove electrons from two water molecules and releases one molecule of oxygen in the last step, the $S_3 \rightarrow [S_4] \rightarrow S_0$ transition (*10*). In the dark, the OEC is dominated by the stable S_1-state. During the S-cycle, four protons are released into the thylakoid lumen. The exact proton release pattern from the $CaMn_4$ cluster is still not completely solved, though protons are released in all steps except in the $S_1 \rightarrow S_2$ transition, which is pH independent (*11*−*13*) and shows no H/D isotope effect (*14*).

In addition to the electron transport, from the OEC via Y_Z, there are several auxiliary electron donors to P_{680}^+. Chlorophyll, carotenoid, and Cytb_{559} can all be oxidized by P_{680}^+ in a pathway that dominates electron transfer under certain conditions (*15*−*18*). This also holds for the reduced form of Y_D (*19*−*22*), which is a redox active tyrosine on the D2 protein (*4*, *5*) localized at a position homologous to the position of Y_Z on the D1 protein. Both tyrosines are probably protonated in the reduced form at physiological pH (*23*, *24*), and EPR spectroscopy indicates that the tyrosines form neutral radicals, $Y-O^\bullet$, after oxidation (*25*, *26*). This implies that the phenolic proton is liberated in connection to electron transfer (PCET). The exact nature of these coupled proton and electron transfer reactions is of significant importance to understand water oxidation and have been extensively studied. The mechanism is still under debate, and it could well be that alternative mechanisms prevail for each tyrosine. The mechanism is also likely to vary with

† The Swedish Research Council, the Swedish Energy Agency, and the Knut and Alice Wallenberg Foundation are acknowledged for financial support.

* Corresponding author. Phone: +46-18-471 65 80. Fax: +46-18-55 98 85. E-mail: stenbjorn.styring@fotomol.uu.se.

[1] Abbrevations: AMPSO, 3-[(1,1-dimethyl-2 hydroxyethyl)amino]-2 hydroxypropane-sulfonic acid; Car, carotenoid; Chl, chlorophyll; Chl_Z, secondary chlorophyll electron donor to P_{680}^+; Cytb_{559}, cytochrome b_{559}; D1 and D2, the core subunits in PSII; DAD, 3,6-diaminodurene; DMSO, dimethyl sulfoxide; EPR, electron paramagnetic resonance; HEPES, *N*-(2-hydroxyethyl)-piperazine-*N*′-2-ethanesulfonic acid; His_D, the histidine on the D2 protein that participates in hydrogen bonding to Y_D; His_Z, the histidine on the D1 protein that participates in hydrogen bonding to Y_Z; MES, 2-[*N*-morpholino] ethanesulfonic acid; OEC, the oxygen-evolving complex; P_{680}, primary electron donor of PSII; PCET, proton coupled electron transfer; P*p*BQ, phenyl-*p*-benzoquinone; PSII, photosystem II; Pheo, the pheophytin acceptor in PSII; Q_A and Q_B, the primary and secondary quinone acceptors in PSII; S-states, intermediates in the cyclic turnover of the OEC; Y_Z, tyrosine 161 (protein sequence numbering in spinach (*1*)) on the D1 subunit; Y_D, tyrosine 161 (protein sequence numbering in spinach (*1*)) on the D2 subunit.

10.1021/bi700377g CCC: $37.00
Published on Web 06/09/2007

the starting S-state, the pH, and the degree of intactness of the OEC. In particular, this is important for the reactions involving Y_Z where structural flexibility and coupled oxidation and deprotonation of the tyrosine opened up for ideas about a direct involvement of Y_Z in water oxidation as a hydrogen atom abstractor from water bound to the $CaMn_4$ cluster (*8*, *9*, *27*). Though an attractive idea, many experiments support another model, often known as the rocking proton model, where the phenolic proton is moving back and forth in a hydrogen bond upon oxidation and reduction, instead of being replaced by a new proton from water as being a prerequisite in the original proposal of the H-atom transfer mechanism. This model was first proposed in ref *28* to explain the very low activation energy of the fast electron transfer from Y_Z to P_{680}^+ in the S_1-state. Y_Z and Y_D are involved in the formation of well-defined hydrogen bonds[2] to His_Z[3] (*29*−*31*) and His_D (*31*−*33*), respectively. In both cases, the histidine provides a good proton acceptor of the phenol proton on tyrosine.

In oxygen-evolving PSII, the oxidation of Y_Z by P_{680}^+ is multiphasic, S-state dependent, and occurs with both ns- and μs-kinetics (*34*). The fast ns-kinetics dominates in the lower S-states (S_0 and S_1) and shows no visible H/D isotope exchange effect (*35*, *36*). In addition, the amplitude of the fast ns-kinetics decreases in the acidic region (*37*, *38*). The very fast kinetics seems to exclude deprotonation of Y_Z to a distant base or in a more loosely defined hydrogen bond network and is suggested to reflect a proton shift in a well-tuned hydrogen bridge between Y_Z-OH and a nearby base, now identified as D1-His190 (His_Z) (*4*, *5*). Significantly slower ns-kinetics is dominating Y_Z oxidation in the higher S-states and is thought to reflect a dielectric relaxation response near Y_Z (*34*, *39*). A much slower μs-component was discovered early (*40*, *41*) and was assigned to centers lacking the $CaMn_4$ cluster (*42*). However, this phase was also found in oxygen-evolving PSII centers (*34*) and was shown to oscillate in size with the S-states (*36*, *43*). The μs-kinetics shows a marked H/D isotope exchange effect, especially in the higher S-states, and is suggested to be coupled to a large scale proton relaxation, involving proton movement in a hydrogen bond network (*36*, *44*).

$Y_D^\bullet$ is stable for hours at room temperature, which for a long time has facilitated its studies by a variety of spectroscopic techniques. The situation is very different for $Y_Z^\bullet$, which is quickly re-reduced from the $CaMn_4$ cluster. The fastest electron donation from the $CaMn_4$ cluster to $Y_Z^\bullet$ occurs in the $S_0 \rightarrow S_1$ transition (30 μs) and is slower in the following transitions (slowest in the $S_3 \rightarrow S_0$ transition; $\tau \sim 1000$ μs) (*45*). This makes the $Y_Z^\bullet$ radical very short-lived in O_2-evolving PSII at normal temperature. The short life time in active PSII is the reason why $Y_Z^\bullet$ mainly has been studied in Ca- or Mn-depleted PSII centers, where the life time of the radical is longer (*46*). However, by removing Ca and/or Mn from the cluster, the microenvironment around Y_Z is changed, which limits the value of studies in such material with respect to gaining an understanding of the molecular function of Y_Z in oxygen-evolving PSII.

It was long unknown that any of the two tyrosines could be oxidized at cryogenic temperature. At these temperatures, many of the components in the charge transfer chain are blocked, including the S-state turnover (*47*) and the electron transfer from Q_A^- to Q_B (*48*). Recently, it has been discovered that almost complete Y_D oxidation could be achieved by illumination at 2−15 K in Mn-depleted PSII at pH 8.5 (*21*, *22*). The pH dependence of $Y_D^\bullet$ formation was fitted with a pK_a of ∼7.6 for a single protonable group (*22*). In intact PSII, there was a parallel discovery that a radical, most likely $Y_Z^\bullet$, could be trapped by illumination at temperatures as low as 5 K. The radical was observed in magnetic interaction with the $CaMn_4$ cluster, giving rise to the so-called split EPR signals (*49*−*51*). Different split EPR signals have now been discovered in all S-states, all originating from magnetic interactions between the $CaMn_4$ and the nearby oxidized radical (S_1 (*49*), S_2 (*52*), S_3 (*53*), and S_0 (*50*)). In this process, it is thought that the $Y_Z^\bullet$ radical is trapped in a semi-stable configuration, and in many cases the split EPR signals decay by recombination with Q_A^- with a half-time of ∼3 min at 5−10 K (*49*, *50*, *54*−*56*).

Thus, for both tyrosines, the oxidation at cryogenic temperature involves mechanisms working when the full electron-transfer chain is blocked. In this way, new spectroscopic probes from both tyrosine radicals, generated by illumination at ultra low temperatures, are now available to investigate the photochemistry of the donor side in PSII and will hopefully provide us with further insight in the complex balance between the different electron donors to P_{680}^+.

In this article, the split EPR signal from the S_1-state has been used to investigate the pH dependence and the mechanism of Y_Z oxidation at cryogenic temperatures. The approach was to induce the Split S_1 signal, originating from the magnetic interaction between the S_1-state and $Y_Z^\bullet$, in intact PSII samples at different pH. By following the Split S_1 signal induction at 5 K versus pH, we could analyze the limitations of $Y_Z^\bullet$ formation. Our results are discussed in the context of literature data for the pH dependence of the S_1- to S_2-state transition (*11*−*13*) and the P_{680}^+ reduction kinetics by Y_Z in intact PSII (*57*), both investigated at physiologically relevant temperatures (∼20 °C). We also studied the competition in electron donation to P_{680}^+ between Y_D and Y_Z in the pH range 4−9 in PSII samples where Y_D was reduced prior to the application of the illumination at low temperature. In these samples, both tyrosines were available as potential donors to P_{680}^+, and Y_D was found to outcompete Y_Z at elevated pH, whereas Y_Z was the preferred electron donor at pH < 7.2.

MATERIALS AND METHODS

PSII Membrane Preparation. PSII enriched membranes (*58*), were prepared from hydroponically grown greenhouse spinach (*Spinacia oleracea*) with modifications according to ref *59*. The storage-buffer was 25 mM MES-NaOH (pH 6.1), 15 mM NaCl, 3 mM $MgCl_2$, and 400 mM sucrose. Chl

[2] Work with mutants and structural analysis of PSII has shown that Y_D forms a hydrogen bond to D2-His190 = His_D (protein sequence numbering in spinach; homologue to D2-His189 in cyanobacteria (*1*, *32*, *33*)), whereas Y_Z forms a hydrogen bond to the homologous D1-His190 = His_Z (cyanobacterial and higher plant numbering (*1*, *29*, *30*)).

[3] We propose here the nomenclature Histidine$_Z$ (His_Z) for the histidine residue on the D1 protein that participates in hydrogen bonding to Y_Z and Histidine$_D$ (His_D) for the histidine residue on the D2 protein that participates in hydrogen bonding to Y_D. The reason is that the exact numbering in the protein sequence of respective histidine residue varies between different organisms (for example, between higher plants, *Euglena* sp., *Chlamydomonas* sp., and cyanobacteria (*1*)).

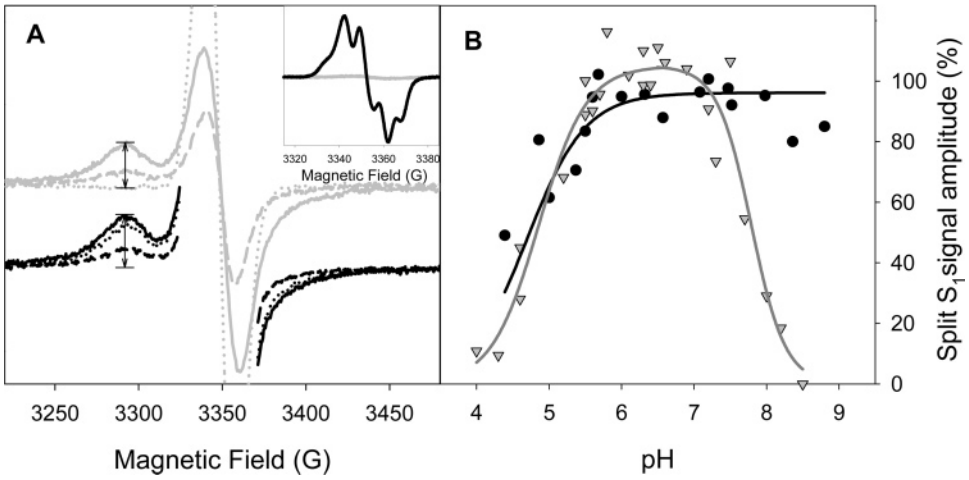

FIGURE 1: The Split S_1 EPR signal was induced by brief illumination at 5 K in PSII samples with Y_D pre-oxidized (black spectra) or pre-reduced (gray spectra). Panel A shows light minus dark difference EPR spectra of the Split S_1 signal measured at pH 4.3 (Y_D^{ox}) and 4.6 (Y_D^{red}) (---), 6.3 (—), and 8.2 (Y_D^{ox}) and 8.5 (Y_D^{red}) (•••). The arrows mark the field position chosen for the signal amplitude measurements in panel B. The inset shows the Y_D radical fully oxidized (black) or reduced (gray) to 1.5% of its original amplitude by the chemical reduction treatment (ascorbate/DAD). Panel B shows the normalized amplitude of the Split S_1 signal plotted vs the bulk pH, both in the presence (black circles) and absence (gray triangles) of Y_D^{ox}. The decrease of the Split S_1 signal at pH < 5.5 could be fitted with a pK_a of ~4.7 (in the presence of Y_D^{ox}; black line) and a pK_a of ~4.9 (in the presence of Y_D^{red}; gray line) for a single protonable group. At pH > 7.5, the amplitude of the Split S_1 signal was high in samples with Y_D^{ox} but decreased with pH in samples with Y_D^{red}. The fit at the high pH side gave a pK_a of ~7.9 for the decrease (gray line). EPR parameters for A and B: temperature 5 K, microwave frequency 9.41 GHz, microwave power 25 mW, and modulation amplitude 10 G. EPR parameters for the inset: temperature 15 K, microwave power 1.0 μW, and modulation amplitude 3.2 G.

determinations were made according to Arnon (*60*). EPR measurements were performed at 2−3 mg Chl/mL.

Chemical Reduction or Photo Oxidation of Y_D. The study was performed in PSII membranes with the redox active Y_D either oxidized or reduced prior to the EPR measurements. $Y_D^•$ was reduced chemically by an ascorbate/DAD treatment in complete darkness (*55*, *61*) to achieve only 1.5−5% remaining $Y_D^•$ (Figure 1A, inset). After two centrifugation steps to remove the reductant, the pellet was suspended to ~3 mg Chl/mL in a low-molar buffer (2 mM MES-NaOH (pH 6.3), 15 mM NaCl, 3 mM $MgCl_2$, and 300 mM sucrose) to facilitate the pH jump. P*p*BQ (1 mM) (dissolved in DMSO, final DMSO 2% (v/v)) was added to the reduced PSII sample before the EPR tubes were filled and rapidly frozen in the dark.

To create PSII samples with Y_D fully oxidized and ready for the pH jump protocol, the BBY particles ([Chl] 1 mg/mL) were washed by centrifugation and resuspended in the low-molar buffer to the final [Chl] of ~3 mg/mL. The PSII membranes were then exposed to room light for 5 min at 20 °C to achieve complete oxidation of Y_D. P*p*BQ (1 mM) (dissolved in DMSO, final DMSO 2% (v/v)) was then added, and EPR tubes were filled in dim green light at 4 °C. The EPR tubes were dark-adapted for 20 min at 4 °C to allow decay of the higher S-states prior to freezing.

pH Jump. The frozen EPR samples, with reduced or oxidized Y_D in the low-molar buffer, were rapidly thawed to 20 °C. Thereafter, the pH was adjusted by addition of a defined buffer (10% v/v) in the pH range 3.3−9.5. The addition and mixing in the EPR tube was made in the dark with a syringe equipped with a spiral, and the sample was immersed, within 20 ± 2 s after the addition, first in an ethanol/dry ice bath and then in liquid N_2. The buffers used were glutamic acid-NaOH (pH 3.3−4.25), MES-NaOH (pH 4.6−6.6), HEPES-NaOH (pH 6.8−7.8), glycylglycine-NaOH (pH 8.0−8.7), and AMPSO (pH 8.8−9.5). The final total buffer concentration in the EPR sample after the addition was 20 mM.

Steady-State Oxygen Evolution. Steady-state oxygen evolution in saturating light at 20 °C was measured with a Clark-type electrode (Hansatech Instruments, U.K.) at 10 μg Chl/mL in a buffer with 25 mM MES-NaOH (pH 6.1), 10 mM NaCl, 10 mM $MgCl_2$, 5 mM $CaCl_2$, and 400 mM sucrose. P*p*BQ (0.5 mM in DMSO) was used as the electron acceptor. Oxygen evolution was 400 ± 50 μmol O_2 (mg Chl)$^{-1}$ h^{-1} and remained constant after the reduction protocol and subsequent washings.

EPR Spectroscopy. Low-temperature EPR measurements were performed in complete darkness with a Bruker ELEXSYS E500 spectrometer using a SuperX EPR049 microwave bridge and a Bruker ST4102 standard cavity. The system was fitted with an Oxford instruments (U.K.) cryostat and temperature controller. The split EPR signals and the other radical EPR signals were induced by illumination for 20 s directly in the cavity at 5 K via a light guide. The light intensity, measured at the position of the sample, was 160 W/m^2 using white light filtered through a 5 cm thick $CuSO_4$ (aq) filter (*55*). Quantification of the non-saturated radical EPR signals from $Y_D^•$ and Car/Chl$^+$ was achieved by double integration of their EPR spectra and comparison to the spectrum from a fully oxidized $Y_D^•$ (1 spin/PSII) measured in the same sample ($Y_D^•$ oxidized) or estimated from the Chl content (in samples with Y_D reduced). We estimate the error in the determination of the radical content to be ±5% because of small errors in both double integration and in the Chl concentration dependence. Double integration was carried out with the Bruker software Xepr. In case the illumination resulted in the formation of both $Y_D^•$ and Car/Chl$^+$, the overlapping spectra were deconvoluted from each other using the Bruker software by weighted subtraction of a spectrum from unperturbed $Y_D^•$.

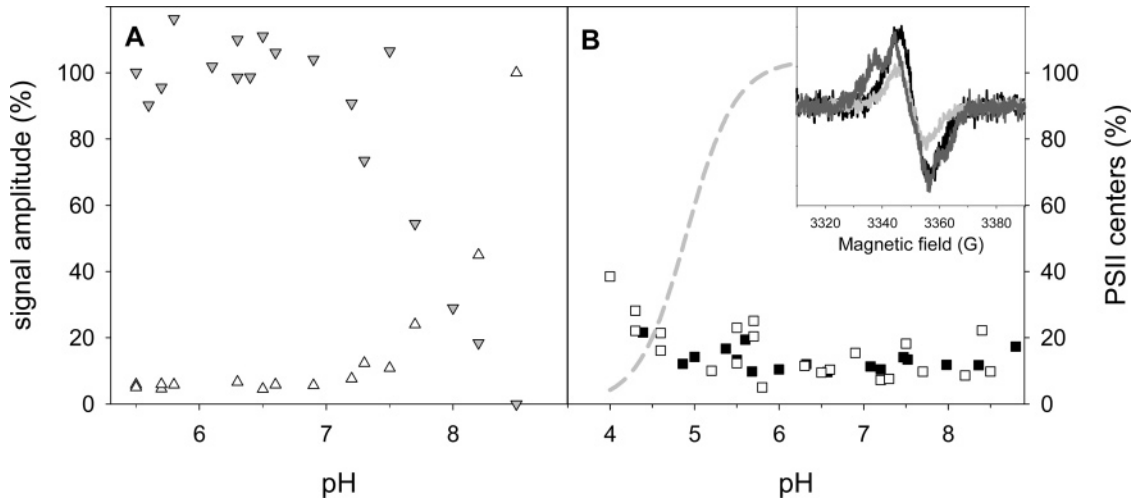

FIGURE 2: The illumination protocol at 5 K also induced EPR signals from other electron donors. In panel A, the oxidation of Y_D (white triangles) in samples with Y_D pre-reduced was followed vs the pH in the same sample as the Split S_1 signal was induced (gray triangles). The oxidation of Y_D increased at pH > 7.5 with an apparent pK_a of ~8, which matched the decrease in split signal amplitude. At pH 8.5, the illumination resulted in a very high degree of Y_D oxidation. Panel B shows the light dependent oxidation at various pH values of a 9−10 G wide radical at g ~2.0026 attributed to Car^+ (black squares, samples with Y_D^{ox}; white squares, samples with Y_D^{red}) measured 7 min after the light was turned off. The increase in the radical signal at low pH is compared to the decrease of the Split S_1 signal amplitude (gray dashed line, fit from Figure 1B). The inset shows the EPR spectra of the light induced EPR signals in the radical region at three different pH values: 4.3 (black), 6.3 (light gray), and 8.2 (dark gray), recorded in samples where Y_D was reduced prior to illumination. EPR parameters for the inset: microwave frequency 9.41 GHz, temperature 5 K, microwave power 1.0 μW, and modulation amplitude 3.2 G.

Integrity of PSII in the pH Treated Sample. After the EPR measurements were concluded, the O_2 evolution, Chl content, and final pH were checked in this order in each individual EPR sample. The O_2 evolution, remaining after the pH jump and EPR measurements, was measured at pH 6.1 (as described above), irrespective of the pH of the EPR sample, within 20 ± 2 s after the sample was thawed (*62*). Swift sample handling was necessary to minimize pH induced damage of the OEC, which occurs quite rapidly in a time dependent manner at elevated pH (*62*). On the high pH side (>8.0), the activity was slightly lowered in some of the samples, and the data points (split signal amplitude) were corrected to full activity. The O_2 evolution was high in all samples included in the results (Figure 1B). Samples where >50% of the original O_2 evolution had been irreversibly lost during the sample handling procedures were judged to be too destroyed to provide reliable information and were excluded from the analysis.

RESULTS

The influence of pH on the formation of the Split S_1 EPR signal at 5 K was studied between pH 4.0−9.0. The light induced Split S_1 signal in intact PSII (Figure 1A) reflects $Y_Z^\bullet$ in magnetic interaction with the $CaMn_4$ cluster in the S_1-state and needs the functional oxidation of Y_Z for its formation (*49*−*51*, *54*, *55*). At normal temperatures (0−20 °C), the S_1 to S_2 state transition, and consequently Y_Z function, has been found to be pH independent (*11*−*13*). The ultralow temperature (5 K) for the induction of the split signal will restrict protein and proton movements. The pH dependence of Y_Z oxidation at 5 K is therefore not necessarily the same as that at room temperature. The experiments were performed in PSII particles with Y_D reduced or oxidized (Figure 1A, inset) prior to split signal induction. In this manner, any competition between the two redox active tyrosines at cryogenic temperature could be revealed.

Figure 1A shows the Split S_1 EPR signal induced in PSII with Y_D reduced (gray line) or oxidized (black line) at different pH. The maximum of the split peak amplitude in both cases was achieved around pH 6.3 and is marked with an arrow in Figure 1A. The dashed and dotted spectra in Figure 1A represent the Split S_1 signal recorded at pH 4.3 (4.6) and 8.2 (8.5), respectively, in PSII samples with Y_D^{ox} (black) or Y_D^{red} (gray). It is clear from the EPR spectra (Figure 1A) that the amplitude recorded at pH 6.3 is quite similar independent of the redox state of Y_D but that the induction of the split signal at high and low pH differs.

Figure 1B shows the pH dependent induction of the Split S_1 signal. In the pH range from 5.5 to 7.0, the formation of the Split S_1 signal is pH independent both with Y_D reduced (gray triangles) and oxidized (black circles). The two curves differ above pH 7.0 and in the presence of Y_D^{ox} (black), the induction of the Split S_1 signal is independent of pH. However, in the presence of Y_D^{red}, the induction of the split signal decreased at pH > 7.0 with an apparent pK_a of 7.9 (gray line, Figure 1B) for one protonable group. In the acidic range at pH < 5.5, the pH dependence is quite similar in the two curves. pH dependence could be fitted with a single protonable group with apparent pK_a values of 4.7 and 4.9 for the decrease of the Split S_1 signal in the acidic pH range in samples with oxidized and reduced Y_D, respectively.

Our brief illumination protocol at 5 K also resulted in the induction of other EPR signals. Similar to earlier observations (*54*, *55*), a small fraction of a featureless radical EPR signal was induced (Figure 2B, inset). At 5 K, the radical predominantly originates from an oxidized carotenoid in the Car/Chl_Z/Cytb_{559} pathway (*15*). (Sometimes, a chlorophyll radical can also contribute to the oxidized species (*18*).) The induction of this radical was pH dependent (Figure 2B). At pH 6.3 (Figure 2B, inset, light gray spectrum), the radical was formed in ~12% of PSII, and this yield was similar between pH 5.0 and 8.5 (Figure 2B). The yield was higher

at lower pH, and it was formed in ~30% of PSII at pH 4.3 with our applied illumination protocol (Figure 2B, inset, black spectrum). This increase of the yield of the Car radical pathway in the acidic pH range (Figure 2B) is probably a result of the inactivation of the electron donor giving rise to the Split S_1 signal (pK_a ~4.7; Figure 1B). No significant difference in the induction of the Car/Chl species between the samples with Y_D oxidized or reduced could be detected in the pH interval studied. It is also noteworthy that we did not observe any significantly increased yield of the radical species at elevated pH in any of the samples (Figure 2B).

The illumination at 5 K also resulted in a pH dependent oxidation of Y_D (Figure 2A) in the samples where Y_D had been pre-reduced. EPR spectra showing the complex, mixed oxidation of the Car/Chl radical and Y_D are shown in the inset in Figure 2B (dark gray spectrum). Below pH 7.2, we observed no oxidation of Y_D (Figure 2A, white triangles), and only carotenoid oxidation was observed. (As described above, this was larger at low pH; Figure 2B.) However, at pH > 7.2, oxidation of Y_D could be observed together with carotenoid oxidation. At pH 8.5, oxidation was very efficient and involved nearly all PSII centers, and $Y_D^{\bullet}$ dominated the resulting EPR spectrum. The oxidation of Y_D was pH dependent and increased with an apparent pK_a ~8.0 (Figure 2A, white triangles). This matches quite well with the pK_a of the decrease of the Split S_1 signal induction observed in the same samples (Figure 2A, gray triangles).

We also followed the oxidation state of Cytb_{559} during illumination at different pH values (not shown). The redox potential and its oxidation state are known to be sensitive to pH (*63*). In our experiments, we could also observe (not shown) that the pH in itself changed the amount and redox forms (high, middle, and low potential) of oxidized Cytb_{559}. On top of these pH induced changes, there occurred some minor photo oxidation (~5−8% of PSII) of the cytochrome by the illumination at 5 K in the entire pH range. This seemed to be less efficient at alkaline pH, but the exact pH dependence could not be determined because of the very small spectral changes involved.

DISCUSSION

In this study, we show that the cryogenic oxidation of Y_Z in the S_1-state is pH dependent. We observe an onset of Y_Z oxidation in the acidic range (pK_a ~4.7), and Y_Z oxidation above this pH is efficient over the entire pH interval studied (pH 5.5−8.8). However, when Y_D is present in the reduced form, it becomes the preferred electron donor at elevated pH (onset of Y_D oxidation with pK_a ~8.0) where it competes efficiently with Y_Z. We will first put our results in relationship to available literature on the pH dependence of the formation of the Split S_1 signal and Y_D oxidation. We will then discuss the interesting, seemingly contradictory, observation that the $S_1 \rightarrow S_2$ transition and consequently the ability to oxidize and reduce Y_Z is pH independent at room temperature (*11*−*13*), whereas we observe a pH dependent shut down of Y_Z oxidation in the acidic pH range at cryogenic temperature. Finally, we will discuss the pH dependent competition between Y_D and Y_Z in intact PSII and explore some mechanistic, molecular proposals to explain our results.

The pH dependent induction of the Split S_1 EPR signal was recently investigated by quite similar procedures (*64*), but both the results and the interpretation of the data differ from ours. The data seemingly indicated that the induction of the Split S_1 signals decreased both in the acidic and the alkaline region. Our results at alkaline pH are very different, and we do not find the inhibition with a pK_a of 7.7 (*64*) when Y_D is oxidized from the start. Instead, we find the induction of the Split S_1 signal to be pH independent between pH 5−8.8. The most likely explanation for this difference lies in the experimental protocol and data handling in the two studies. At alkaline pH, the $CaMn_4$ cluster is prone to pH dependent damage, often accompanied by an irreversible release of Mn. This damage is pH and time dependent, occurring faster at higher pH. In our pH study, we try to manage this by a swift handling of the samples *after* the pH swap (*62*), where the samples are frozen 20 ± 2 s after the first buffer addition. Despite this quite fast freezing, the $CaMn_4$ cluster is destroyed in a fraction of the centers, leading to partial loss of oxygen evolution at high pH. However, these centers are not even candidates for the formation of the Split S_1 signal because the $CaMn_4$ cluster (necessary for the split signal formation) is lost. These centers must therefore be removed from the analysis of the pH dependence of the Split S_1 signal. We handle this loss of potential Split S_1 signal-forming centers by measuring the remaining oxygen evolution (swiftly after thawing the EPR sample and by bringing it back to pH 6.1; see Materials and Methods). We then compensated for the lost PSII centers by plotting the fraction of centers forming the Split S_1 signal (Figures 1 and 2), thereby only investigating samples that still have a complete $CaMn_4$ cluster and eliminating "false split" signal inhibition coming from centers where the $CaMn_4$ cluster was destroyed. Zhang (*64*) does not report on the control of remaining O_2 evolution activity after the pH swap, which was performed slower (30 s) in his study. Therefore, a possible explanation of the discrepancy between the data here and that in ref *64* is that the pK_a on the alkaline pH side reported in ref *64* reflects a large fraction of PSII where the OEC was lost because of the high pH and longer incubation time used instead of, as proposed, the inhibition of the formation of the Split S_1 signal from pH dependent mechanistic reasons.

We also disagree on the interpretation of the reported decrease of the Split S_1 signal induction at acidic pH (pK_a ~ 4.7). In ref *64*, the acidic pK_a is interpreted as the inactivation of oxygen evolution in PSII and not immediately connected to the Y_Z oxidation. First, we argue that the cryogenic oxidation of Y_Z to form the Split S_1 signal is more related to the oxidation of Y_Z and thus preceding the oxidation of the $CaMn_4$ cluster in the $S_1 \rightarrow S_2$ transition. It is thus not connected to the pH dependent inhibition of oxygen evolution, which has been shown to be dominated by a pH dependent inhibition of the $S_3 \rightarrow S_0$ transition (*12*). In contrast, the $S_1 \rightarrow S_2$ transition has been found to occur with a pH independent efficiency between pH 4−9 (*11*−*13*). This clearly shows that Y_Z oxidation at room temperature is indeed possible in the region pH 4−5. In contrast, the Split S_1 signal induction is strongly inhibited, suggesting that Y_Z cannot be oxidized at 5 K. We therefore judge that the acidic inhibition of Split S_1 signal formation reports on the molecular structure in the direct environment of Y_Z and will discuss some molecular possibilities for this process. An alternative interpretation is that low pH could partially inhibit

the $CaMn_4$ cluster, potentially by removal of the Ca^{2+} ion. To control this, the oxygen evolution remaining after the pH swap to the acidic region was measured at pH 6.1. If needed, the Split S_1 signal was corrected for the loss of oxygen evolution in the sample. However, this irreversible inhibition of oxygen evolution was much less in the acidic pH range (not shown) than in the samples exposed to the alkaline pH jump, making the necessary correction very small. In addition, most procedures for Ca^{2+} depletion involve treatment at pH < 3.5 in the presence of chelators such as citrate for prolonged periods of time (compared to the 20 ± 2 s allowed in our present study). We therefore conclude that the acidic inhibition of the Split S_1 signal formation we observed with pK_a 4.7−4.9 (Figure 1B) did not involve any irreversible destruction of the OEC. Instead, the explanation for the difference in the behavior of Y_Z oxidation at room temperature and cryogenic temperature most probably should be found at the molecular level.

We have investigated the pH dependence of the competition between the two redox active tyrosines by using the Split S_1 signal, which is a novel EPR probe reporting on Y_Z oxidation in intact PSII. By keeping Y_D reduced before the illumination at 5 K, we could study the low-temperature oxidation of both Y_D and Y_Z in the same sample. It can be concluded that Y_D is the preferred electron donor to P_{680}^+ at elevated pH (pK_a ~8) because the formation of $Y_D^\bullet$ increased at the expense of the Split S_1 signal, which decreased with pK_a ~7.9. A first report on the competition between Y_Z (Z) and Y_D (D) at high pH was published by Boussac and Etienne (*65*). They found an equilibrium constant between Z^+D and ZD^+ at pH 8.5 in tris-washed chloroplasts, but the connection between Z and D was looser at lower pH. Our study here is the first investigation in intact, oxygen-evolving PSII of competition between the two redox active tyrosines at cryogenic temperatures. (An early related study directly following the kinetics and amplitude of Y_D oxidation in intact PSII between pH 4.5−8.3 was performed at 21 °C (*66*).) However, Faller et al. (*22*) investigated the pH dependence of the oxidation of Y_D at cryogenic temperatures in Mn-depleted PSII from both cyanobacteria and plants and found an onset of Y_D oxidation with a pK_a of ~7.6 for a single protonable group. This was proposed to correlate to an unexpected fast oxidation ($t_{1/2}$ = 190 ns) of Y_D at room temperature that was controlled by a pK_a of ~7.7 (*20*), indicating a relationship between ns-kinetics for Y_D providing electrons to P_{680}^+ at room temperature and the ability to oxidize Y_D at cryogenic temperature. Mechanistic explanations behind this efficient oxidation of Y_D at elevated pH have been extensively discussed by Faller et al. (*20*−*22*). The formation of the tyrosine radical, that can occur as low as 1.8 K, has been proposed to involve either proton coupled electron transfer through tunneling of the phenolic proton in a hydrogen bond to His_D or pure electron transfer where Y_D is a tyrosinate (Y_D-O^-) from start (*20*−*22*). This issue was addressed with high magnetic field spectroscopy (*21*), and it was found that the $Y_D^\bullet$ radical induced at 1.8 K was a high energy radical intermediate trapped in an electropositive environment, probably reflecting the presence of a proton in the hydrogen bond. From this analysis, proton coupled electron transfer was favored.

In intact PSII, investigated at room temperature, a proton binding with a pK_a 7.3−7.5 was found to retard the electron transfer from Y_D to the $CaMn_4$ cluster, presumably via redox equilibria involving P_{680} and Y_Z (*66*). The pK_a was interpreted to reflect a base in the vicinity of Y_D, which then was already suggested to be His_D (*66*). In this mechanism, proton binding to His_D at pH < 7.3−7.5 destroys the well-tuned hydrogen bond and shifts the system to allow only slower Y_D oxidation to occur. Under these circumstances, oxidation of the tyrosine and its coupled deprotonation will demand that more extensive proton and protein movements proceed. This type of mechanism would be frozen out at cryogenic temperature (5 K), which would explain why we observe no Y_D oxidation below pH 7.2. Oxidation of Y_D in this situation would also be too slow to compete with Y_Z for electron donation to P_{680}^+, at least when pH < pK_a for His_D.

Our results are fully compatible with these studies and confirm that Y_D is the preferred donor to P_{680}^+ at higher pH and also in the presence of a functional OEC. In the remaining pH interval studied (pH 4−7), Y_Z is the dominating donor, and we observed no oxidation of Y_D. Our results here contribute further input to these discussions and show that Y_D out-competes Y_Z at higher pH in PSII with an intact OEC where the environment of Y_Z is not disturbed and where Y_Z is known to work much faster than in the Mn-depleted systems studied by Faller et al. (*20*−*22*).

The reason why Y_D wins over Y_Z at elevated pH in a situation when both tyrosines are available for electron donation should be sought in their different redox potentials and in the microenvironment of their immediate surroundings. It has long been known that Y_Z is 200−250 mV more oxidizing than Y_D around neutral pH (*66*), and these early kinetic measurements were recently supported by theoretical calculations based on the X-ray structures of PSII (*67*). To a large extent, this higher redox potential reflects the location of the $CaMn_4$ cluster in the close vicinity of Y_Z. Therefore, Y_D will be easier to oxidize from P_{680}^+ once the well-tuned hydrogen bond is set. In addition, the environment between P_{680} and Y_D is more hydrophobic than that between P_{680} and Y_Z. This was suggested in computer modeling work of the PSII core (*1*) and was verified in the X-ray structures (*4*, *5*). The effect on these different dielectrics on the electrostatic interactions between P_{680}^+ and the two tyrosines was recently discussed in theoretical work (*67*), and it was concluded that Y_D was much more sensitive to the redox state of P_{680} than Y_Z.

An interesting question relates to why Y_Z oxidation at 5 K is activated with pK_a 4.7−4.9 (Figure 1B), while Y_D oxidation is activated with pK_a 7.6−8.0 (Figure 2A (*20*−*22*)). It is likely that the pH dependent onset of Y_Z oxidation reflects the establishment of a well-defined hydrogen bond involving the phenolic proton on Y_Z most probably to His_Z, similar to what has been proposed for Y_D and His_D (see below; (*20*−*22*)). If this holds true, then the hydrogen bond involving Y_Z is formed at lower pH compared to that for Y_D (compare pK_a of 4.7 for Split S_1 signal formation and pK_a ~8 for Y_D oxidation). This difference has been observed before, and there are several observations of p$K_a$values involving Y_Z and Y_D oxidation similar to those found here. In an early study on Y_D in intact PSII, Vass and Styring observed a pK_a of 7.3−7.5 (*66*), which was suggested to reflect the titration of His_D. The lower pK_a for steering the oxidations in the water-oxidizing branch on the donor side of PSII was first observed in optical studies (*68*), where a pK_a of 5.3 was found to retard the electron transfer from Y_Z

to P_{680}^+, and this pK_a was later verified in detailed comparative studies of the electron transfer between Y_Z and P_{680}^+ in both intact and Mn-depleted PSII (*46*).

Taken together, these results imply that protonation of one (or several) group(s) in the vicinity break the well-tuned hydrogen bond between Y_Z and His_Z. Which group titrates with pK_a ~4.7 cannot be known for certain, but candidates involve His_Z itself, a water molecule in the vicinity, or D1-Asn298 that seemingly participates in the hydrogen bond network around Y_Z and His_Z (*67*). If direct titration of His_Z is responsible, then it seems that His_Z and His_D titrates with pK_a values differing by as much as 3 pH units. There are probably multiple reasons for this, but one likely important factor is the presence of the $CaMn_4$ cluster only a few Ångströms away from the Y_Z/His_Z couple, which is likely to significantly lower the pK_a of neighboring bases. An alternative explanation to titration of the histidine could be direct titration of Y_Z forming the tyrosinate, limiting the oxidation of Y_Z to a pure electron transfer reaction at physiological pH. This is supported by optical difference spectra, suggesting that the phenolic proton is shifted toward a base in a hydrogen bond already in the reduced state (*69*). If the pK_a of ~4.7 involved direct titration of Y_Z-OH, then this would be abnormally low pH (normally tyrosines titrate with pK_a ~10), which we find unlikely. In addition, there are several arguments in favor of the pK_a 4.7 reflecting the titration of the base (His_Z) instead of the tyrosine. FTIR studies have shown that Y_Z is protonated in the reduced state at pH 6 in both Mn-depleted PSII (*24*) and in intact PSII. In addition, Noguchi et al. (*23*) found a protonated tyrosine coupled to the $CaMn_4$ cluster. If not already deprotonated, Y_Z would require deprotonation upon oxidation to form the neutral radical ($Y_Z^\bullet$) (*25*, *26*). Y_Z oxidation demands a hydrogen bonded base (His_Z), and protonation of this base would remove the ability to form the crucial hydrogen bond. Thus, our pK_a of ~4.7 could reflect the titration of the hydrogen bond partner (probably His_Z), whereas a pK_a of 8.5 has been assigned to the direct titration of Y_Z in intact PSII (*70*). Although both p$K_a$values are strongly tuned by the protein, the relative pK_a difference (4 pH units) is the same as that for the free amino acids.

The efficiency, following a single flash, of the $S_1 \rightarrow S_2$ state transition measured at the level of the $CaMn_4$ cluster is pH independent at room temperature in the interval pH 4.1−8.4 studied by EPR (*12*) and pH 3.5−9.5 studied by FTIR (*13*). Thus, Y_Z is operational in the whole pH range used in this study, although Y_Z reduces P_{680}^+ with slower kinetics at lower pH (*36*, *37*, *44*). Our investigation describes a decrease of the Split S_1 signal induction at 5 K (i.e., Y_Z oxidation) in the acidic pH range (pK_a ~ 4.7−4.9) for PSII in the S_1-state, which at first glance could seem contradictory to the room-temperature data (*12*, *13*). To explain the apparent discrepancy, we must consider the extremely low temperature used to induce the Split S_1 signal. At 5 K, charge separation occurs in PSII, but the electron transfer is blocked on the acceptor side at the level of Q_A^-. On the donor side, all steps involving the $CaMn_4$ cluster, including the $S_1 \rightarrow S_2$ transition, are inhibited already at much higher temperatures than 5 K (*47*). It can therefore be concluded that the difference between the low-temperature and the room-temperature data must be sought at the level of Y_Z, probably reflecting a temperature and pH dependent oxidation of the tyrosine. A plausible cause is that the oxidation of Y_Z at room temperature involves different mechanisms that dominate in different pH intervals. In this case, our results can be explained if the mechanism that is favored at low pH is limited (frozen out) by the very low temperature used in the induction of the Split S_1 signal, while the mechanism(s) dominating at physiological and elevated pH would remain functional at cryogenic temperature. One likely scenario is that the oxidation of Y_Z at 5 K (pH > pK_a 4.7) does not involve major proton or protein movements, whereas Y_Z oxidation at acidic pH might involve proton or side chain reorganizations that are not possible at cryogenic temperature. A mechanistic proposal incorporating these elements is presented in Scheme 1 and is discussed below.

Photo-oxidation of Y_D or Y_Z is considered to result in the formation of the neutral oxidized tyrosine radical (*25*, *26*). Consequently, oxidation is coupled to deprotonation of the phenolic proton. For both tyrosines, deprotonation probably occurs in a hydrogen bond to the nearby histidine residue (*2*). Scheme 1 shows the proposed situation around Y_Z and His_Z above (left) and below (right) the pK_a of the histidine. Above the pK_a, the histidine is available for hydrogen bonding to the tyrosine (Scheme 1, left), while this is not the case below pK_a for the histidine (Scheme 1, right). In this case, it is instead probable that the tyrosine is involved in one or several hydrogen bonds to other proton acceptors, B, that can deprotonate Y_Z when His_Z is protonated. There are several candidates for B, including a water molecule placed between Y_Z and the Ca^{2+} as suggested in ref *67* or an amino acid side chain in the close vicinity. An interesting candidate for the latter is D1-Gln165. Common for all candidates is that the weaker H bond to the phenolic proton from Y_Z does not allow proton movement at 5 K and consequently light driven oxidation of the tyrosine.

In the S_1-state, the major reduction of P_{680}^+ by Y_Z occurs in the ns-time scale at physiological conditions (*28*, *34*, *38*). This kinetics has a very low activation energy (~10 kJ/mol (*28*)) and shows virtually no kinetic H/D-isotope effect (*35*, *38*). It has been interpreted as oxidation of Y_Z with the proton moving in a well-established hydrogen bond to a base (*28*) now identified as His_Z (*4*, *5*, *29*−*31*, *71*). This ns-component of the P_{680}^+ reduction kinetics is pH independent between pH 5.5 and 8.0 (*37*, *38*) and shows no deuterium isotope effect (*35*), reflecting that no proton leaves the system. The amplitude of the fast ns-kinetics decreased at lower pH with a pK_a of ~4.5−4.6 (*37*, *38*, *46*, *72*). This is remarkably similar to the cryogenic induction of the Split S_1 signal described here, which was pH independent between pH 5.5−8.8, but was inhibited with pK_a ~4.7 in the acidic range. It is thus highly likely that both effects reflect the same phenomenon, and we propose that both the fast ns kinetics at room temperature and the cryogenic oxidation of Y_Z demand that the phenolic proton is able to move in a well-tuned hydrogen bond.

At lower pH, cryogenic oxidation of Y_Z is not possible (Figure 1B), whereas Y_Z oxidation is still feasible at room temperature. However, it occurs with slower kinetics in the nanosecond time range and with a dominating fraction of Y_Z oxidation occurring with μs-kinetics (*37*, *46*). The latter phase also shows a significant H/D isotope effect (*36*, *38*), reflecting that the reaction must involve extensive movements of one or more protons. There can be several reasons for

Scheme 1: Model Explaining the Hydrogen Bond Properties and Oxidative Reactions Involving Y_Z at 5 K at pH < pK_{His-Z} (right) and pH > pK_{His-Z} (left)[a]

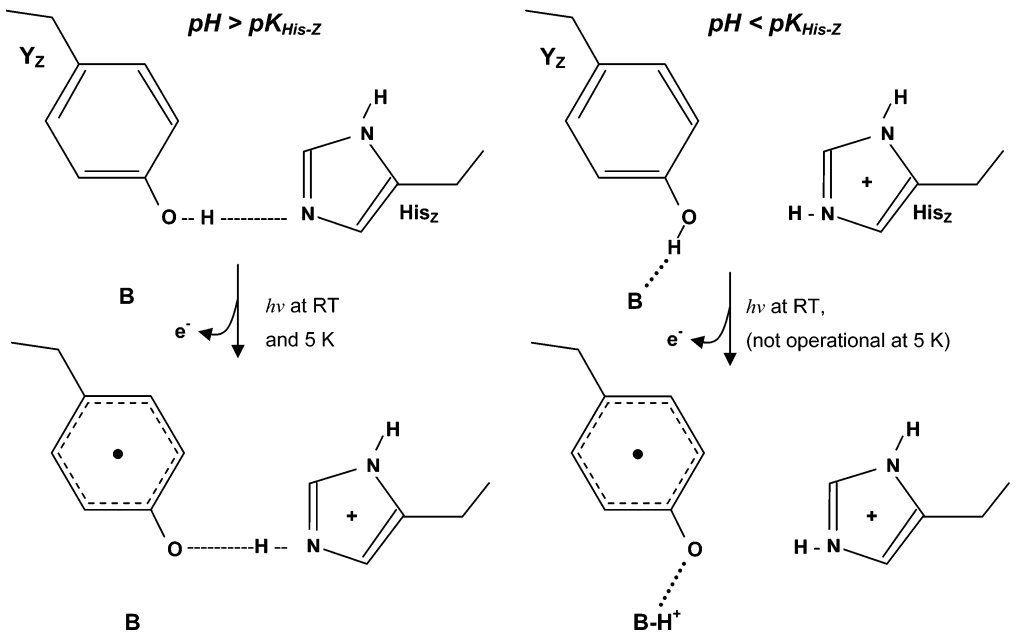

[a] The left-hand box describes the situation when the Split S_1 signal can be formed. Before illumination at 5 K, Tyr161 forms a well-tuned H-bond to the neighboring His190 on the D1 protein via the phenolic proton to the nitrogen in the imidazole ring. Following illumination at 5 K, Y_Z is able to reduce P_{680}^+, only if the phenolic proton leaves the tyrosine in a well-tuned hydrogen bond forming the neutral $Y_Z^\bullet$ radical. The depicted hydrogen bond fulfills this demand in the case when pH > pK_{His-Z}. In the right-hand box, the situation is shown when the histidine is protonated at pH < pK_{His-Z}. In this case, the tyrosine can no longer be deprotonated at 5 K via the H-bond to the histidine. The result is that oxidation of Y_Z and, consequently, split S_1 signal formation is prevented at 5 K. It is likely that Y_Z can still deprotonate but in less well set hydrogen bonds to alternative bases (B), which allows Y_Z to function in slower but still efficient electron transfer at room temperature (RT) where more elaborate hydrogen movements are allowed.

this, but the mechanism behind it is likely to reflect that the phenolic proton is no longer involved in the well-tuned hydrogen bond to His_Z. The same mechanism was previously suggested to explain the decrease of the ns-kinetics at low pH (*72*). Instead, the phenolic proton is probably involved in one or several hydrogen bonds to more distant bases or to a less well-defined proton network, potentially involving water molecules and side chains in the vicinity, and deprotonates there over a longer distance (Scheme 1, right). This is very unlikely to occur at liquid helium temperature, thereby preventing the formation of the Split S_1 signal.

At optimal pH for oxygen evolution, there is a rather small fraction of PSII centers where the hydrogen bond is not well defined. In this small fraction of centers, Y_Z oxidation at ambient temperature is much slower and occurs in microseconds in an isotope dependent manner (*36*, *44*). Presumably, Y_Z in these latter PSII centers is also unable to undergo oxidation at 5 K because of its inability to deprotonate at the low temperature. In those centers, other donors are likely to become active, probably being reflected in the always present, but rather small and pH dependent (Figure 2B) oxidation of the Car/Chl_Z/Cytb_{559}. Our results also report on the oxidation of these other electron donors in PSII. Illumination at low temperature always results in fractional oxidation of some of the components of the Car/Chl_Z/Cytb_{559} pathway (*15*, *16*, *18*) accompanying the formation of the Split S_1 signal (*49*, *54*, *55*). In this study, a pH independent formation of 10−12% of a radical, probably Car^+, was observed at pH > 5. At lower pH, when neither Y_Z nor Y_D could provide electrons to P_{680}^+, an increased yield of the EPR signal from Car^+ was observed after cryogenic illumination (Figure 2B). This reflects that the probability for electron donation from the Car/Chl_Z/Cytb_{559} pathway increased when the main donation pathways from Y_Z and/or Y_D were closed down. It is worth pointing out that the same pattern was found irrespective of the redox state of Y_D. At high pH, there was no increase in the Car^+ signal because here, either the Split S_1 signal was formed or Y_D was oxidized upon illumination at 5 K in samples where Y_D was pre-reduced.

The presence of oxidized $Y_D^\bullet$ has been proposed to steer the redox potential of P_{680}/P_{680}^+ and direct its oxidizing power to the chlorophyll moiety that is located on the D1 protein closest to Y_Z (*73*). Therefore, the presence of $Y_D^\bullet$ would help to facilitate fast electron transfer from Y_Z to P_{680}^+. It has, however, been shown that the contribution from $Y_D^\bullet$ to the redox potential of P_{680}/P_{680}^+ is very small, and only a slight shift in the position of the cation on P_{680}^+ closer to P_A has been observed (*74*). In the Y160F mutant, the lack of $Y_D^\bullet$ has a slight effect on the immediate surroundings and on P_{680}, although the redox properties of P_{680} were not significantly tuned (*75*). Moreover, an important electrostatic role of Y_D would require that when Y_D is reduced prior to illumination, the first charge separation would generate $Y_D^\bullet$. Only thereafter would the catalytic pathway involving Y_Z and the $CaMn_4$ cluster become active. Our data indicate that this at least is not true at pH < pK_{His-D} (Figure 2A) and 5 K, where we observe the exclusive formation of the Split S_1 signal, while Y_D remains reduced upon illumination. In contrast, at pH > pK_{His-D}, Y_D becomes the preferred electron donor and wins in situations where it competes with Y_Z. An explanation for this lack of electrostatic effect in PSII at

physiological pH ($<pK_{His-D}$) could be that His_D is already protonated. At higher pH, we cannot rule out an electrostatic influence.

ACKNOWLEDGMENT

Valuable discussions with miss T. Irebo, Drs. F. Mamedov, F. Ho, L. Hammarström, J. Su, and A. Thapper are gratefully acknowledged.

REFERENCES

1. Svensson, B., Vass, I., and Styring, S. (1991) Sequence analysis of the D1 and D2 reaction center proteins of photosystem II, *Z. Naturforsch., C: Biosci. 46*, 765−776.
2. Barber, J. (2003) Photosystem II: The engine of life, *Q. Rev. Biophys. 36*, 71−89.
3. Nelson, N., and Yocum, C. F. (2006) Structure and function of photosystems I and II, *Annu. Rev. Plant Biol. 57*, 521−565.
4. Loll, B., Kern, J., Saenger, W., Zouni, A., and Biesiadka, J. (2005) Towards complete cofactor arrangement in the 3.0 Å resolution structure of photosystem II, *Nature 438*, 1040−1044.
5. Ferreira, K. N., Iverson, T. M., Maghlaoui, K., Barber, J., and Iwata, S. (2004) Architecture of the photosynthetic oxygen-evolving center, *Science 303*, 1831−1838.
6. Biesiadka, J., Loll, B., Kern, J., Irrgang, K.-D., and A, Z. (2004) Crystal structure of cyanobacterial photosystem II at 3.2 Å resolution: a closer look at the Mn-cluster, *Phys. Chem. Chem. Phys. 6*, 4733−4736.
7. Yano, J., Kern, J., Sauer, K., Latimer, M. J., Pushkar, Y., Biesiadka, J., Loll, B., Saenger, W., Messinger, J., Zouni, A., and Yachandra, V. K. (2006) Where water is oxidized to dioxygen: structure of the photosynthetic Mn_4Ca cluster, *Science 314*, 821−825.
8. Hoganson, C. W., and Babcock, G. T. (1997) A metalloradical mechanism for the generation of oxygen from water in photosynthesis, *Science 277*, 1953−1956.
9. Tommos, C., and Babcock, G. T. (1998) Oxygen production in nature: A light-driven metalloradical enzyme process, *Acc. Chem. Res. 31*, 18−25.
10. Kok, B., Forbush, B., and McGloin, M. (1970) Cooperation of charges in photosynthetic O_2 evolution-I. A linear four step mechanism, *Photochem. Photobiol. 11*, 457−475.
11. Damoder, R., and Dismukes, G. C. (1984) pH dependence of the multiline, manganese EPR signal for the 'S_2' state in PS II particles. Absence of proton release during the S_1—S_2 electron transfer step of the oxygen evolving system, *FEBS Lett. 174*, 157−161.
12. Bernat, G., Morvaridi, F., Feyziyev, Y., and Styring, S. (2002) pH dependence of the four individual transitions in the catalytic S-cycle during photosynthetic oxygen evolution, *Biochemistry 41*, 5830−5843.
13. Suzuki, H., Sugiura, M., and Noguchi, T. (2005) pH dependence of the flash-induced S-state transitions in the oxygen-evolving center of photosystem II from *Thermosynechoccocus elongatus* as revealed by Fourier transform infrared spectroscopy, *Biochemistry 44*, 1708−1718.
14. Haumann, M., Hundelt, M., Jahns, P., Chroni, S., Bogershausen, O., Ghanotakis, D., and Junge, W. (1997) Proton release from water oxidation by photosystem II: similar stoichiometries are stabilized in thylakoids and PSII core particles by glycerol, *FEBS Lett. 410*, 243−248.
15. Hanley, J., Deligiannakis, Y., Pascal, A., Faller, P., and Rutherford, A. W. (1999) Carotenoid oxidation in photosystem II, *Biochemistry 38*, 8189−8195.
16. Tracewell, C. A., Cua, A., Stewart, D. H., Bocian, D. F., and Brudvig, G. W. (2001) Characterization of carotenoid and chlorophyll photooxidation in photosystem II, *Biochemistry 40*, 193−203.
17. Mamedov, F., and Styring, S. (2003) Logistics in the life cycle of photosystem II: lateral movement in the thylakoid membrane and activation of electron transfer, *Physiol. Plant. 119*, 328−336.
18. Frank, H. A., and Brudvig, G. W. (2004) Redox functions of carotenoids in photosynthesis, *Biochemistry 43*, 8607−8615.
19. Magnuson, A., Rova, M., Mamedov, F., Fredriksson, P. O., and Styring, S. (1999) The role of cytochrome b559 and $tyrosine_D$ in protection against photoinhibition during in vivo photoactivation of photosystem II, *Biochim. Biophys. Acta 1411*, 180−191.
20. Faller, P., Debus, R. J., Brettel, K., Sugiura, M., Rutherford, A. W., and Boussac, A. (2001) Rapid formation of the stable tyrosyl radical in photosystem II, *Proc. Natl. Acad. Sci. U.S.A. 98*, 14368−14373.
21. Faller, P., Goussias, C., Rutherford, A. W., and Un, S. (2003) Resolving intermediates in biological proton-coupled electron transfer: a tyrosyl radical prior to proton movement, *Proc. Natl. Acad. Sci. U.S.A. 100*, 8732−8735.
22. Faller, P., Rutherford, A. W., and Debus, R. J. (2002) Tyrosine D oxidation at cryogenic temperature in photosystem II, *Biochemistry 41*, 12914−12920.
23. Noguchi, T., Inoue, Y., and Tang, X. S. (1997) Structural coupling between the oxygen-evolving Mn cluster and a tyrosine residue in photosystem II as revealed by Fourier transform infrared spectroscopy, *Biochemistry 36*, 14705−14711.
24. Berthomieu, C., Hienerwadel, R., Boussac, A., Breton, J., and Diner, B. A. (1998) Hydrogen bonding of redox-active tyrosine Z of photosystem II probed by FTIR difference spectroscopy, *Biochemistry 37*, 10547−10554.
25. Force, D. A., Randall, D. W., Britt, R. D., Tang, X. S., and Diner, B. A. (1995) ^2H ESE-ENDOR study of hydrogen bonding to the tyrosine radicals Y_D' and Y_z' of Photosystem II, *J. Am. Chem. Soc. 117*, 12643−12644.
26. Tommos, C., Tang, X. S., Warncke, K., Hoganson, C. W., Styring, S., McCracken, J., Diner, B. A., and Babcock, G. T. (1995) Spin-density distribution, conformation, and hydrogen-bonding of the redox-active tyrosine Y_Z in photosystem II from multiple electron magnetic-resonance spectroscopies: Implications for photosynthetic oxygen evolution, *J. Am. Chem. Soc. 117*, 10325−10335.
27. Hoganson, C. W., Lydakis-Simantiris, N., Tang, X. S., Tommos, C., Warncke, K., Babcock, G. T., Diner, B. A., McCracken, J., and Styring, S. (1995) A hydrogen-atom abstraction model for the function of Y_Z in photosynthetic oxygen evolution, *Photosynth. Res. 46*, 177−184.
28. Eckert, H. J., and Renger, G. (1988) Temperature-dependence of $P680^+$ reduction in O_2-evolving PS II membrane-fragments at different redox states S_i of the water oxidizing system, *FEBS Lett. 236*, 425−431.
29. Mamedov, F., Sayre, R. T., and Styring, S. (1998) Involvement of histidine 190 on the D1 protein in electron/proton transfer reactions on the donor side of photosystem II, *Biochemistry 37*, 14245−14256.
30. Hays, A. M. A., Vassiliev, I. R., Golbeck, J. H., and Debus, R. J. (1998) Role of D1-His190 in proton-coupled electron transfer reactions in photosystem II: a chemical complementation study, *Biochemistry 37*, 11352−11365.
31. Svensson, B., Vass, I., Cedergren, E., and Styring, S. (1990) Structure of donor side components in photosystem II predicted by computer modelling, *EMBO J. 9*, 2051−2059.
32. Tommos, C., Davidsson, L., Svensson, B., Madsen, C., Vermaas, W., and Styring, S. (1993) Modified EPR spectra of the $tyrosine_D$ radical in photosystem II in site-directed mutants of *Synechocystis sp. PCC 6803*: identification of side chains in the immediate vicinity of $tyrosine_D$ on the D2 protein, *Biochemistry 32*, 5436−5441.
33. Tang, X. S., Chisholm, D. A., Dismukes, G. C., Brudvig, G. W., and Diner, B. A. (1993) Spectroscopic evidence from site-directed mutants of *Synechocystis PCC6803* in favor of a close interaction between histidine 189 and redox-active tyrosine 160, both of polypeptide D2 of the photosystem II reaction center, *Biochemistry 32*, 13742−13748.
34. Brettel, K., Schlodder, E., and Witt, H. T. (1984) Nanosecond reduction kinetics of photooxidized chlorophyll-a_{II} (P-680) in single flashes as a probe for the electron pathway, H^+-release and charge accumulation in the O_2-evolving complex, *Biochim. Biophys. Acta 766*, 403−415.
35. Karge, M., Irrgang, K. D., Sellin, S., Feinaugle, R., Liu, B., Eckert, H. J., Eichler, H. J., and Renger, G. (1996) Effects of hydrogen deuterium exchange on photosynthetic water cleavage in PS II core complexes from spinach, *FEBS Lett. 378*, 140−144.
36. Schilstra, M. J., Rappaport, F., Nugent, J. H. A., Barnett, C. J., and Klug, D. R. (1998) Proton/hydrogen transfer affects the S state-dependent microsecond phases of $P680^+$ reduction during water splitting, *Biochemistry 37*, 3974−3981.
37. Schlodder, E., and Meyer, B. (1987) pH-dependence of oxygen evolution and reduction kinetics of photooxidized chlorophyll-a_{II}

(P-680) in photosystem II particles from *Synechococcus* sp., *Biochim. Biophys. Acta 890*, 23−31.
38. Christen, G., Seeliger, A., and Renger, G. (1999) $P680^{+\bullet}$ reduction kinetics and redox transition probability of the water oxidizing complex as a function of pH and H/D isotope exchange in spinach thylakoids, *Biochemistry 38*, 6082−6092.
39. Mulkidjanian, A. Y. (1999) Photosystem II of green plants: on the possible role of retarded protonic relaxation in water oxidation, *Biochim. Biophys. Acta 1410*, 1−6.
40. Gläser, M., Wolff, C., Buchwald, H. E., and Witt, H. T. (1974) On the photoactive chlorophyll reaction in system II of photosynthesis. Detection of a fast and large component, *FEBS Lett. 42*, 81−85.
41. Conjeaud, H., Mathis, P., and Paillotin, G. (1979) Primary and secondary electron donors in photosystem II of chloroplasts. Rates of electron transfer and location in the membrane, *Biochim. Biophys. Acta 546*, 280−291.
42. Hoganson, C. W., Casey, P. A., and Hansson, Ö. (1991) Flash-photolysis studies of manganese-depleted photosystem-II: evidence for binding of Mn^{2+} and other transition-metal ions, *Biochim. Biophys. Acta 1057*, 399−406.
43. Christen, G., Reifarth, F., and Renger, G. (1998) On the origin of the '35-μs kinetics' of $P680^{+\bullet}$ reduction in photosystem II with an intact water oxidising complex, *FEBS Lett. 429*, 49−52.
44. Christen, G., and Renger, G. (1999) The role of hydrogen bonds for the multiphasic $P680^{+\bullet}$ reduction by Y_Z in photosystem II with intact oxygen evolution capacity. Analysis of kinetic H/D isotope exchange effects, *Biochemistry 38*, 2068−2077.
45. Hoganson, C. W., and Babcock, G. T. (1988) Electron-transfer events near the reaction center in O_2-evolving photosystem-II preparations, *Biochemistry 27*, 5848−5855.
46. Ahlbrink, R., Haumann, M., Cherepanov, D., Bogershausen, O., Mulkidjanian, A., and Junge, W. (1998) Function of tyrosine Z in water oxidation by photosystem II: electrostatical promotor instead of hydrogen abstractor, *Biochemistry 37*, 1131−1142.
47. Styring, S., and Rutherford, A. W. (1988) Deactivation kinetics and temperature-dependence of the S-state transitions in the oxygen-evolving system of photosystem II measured by EPR spectroscopy, *Biochim. Biophys. Acta 933*, 378−387.
48. Joliot, P., and Joliot, A. (1973) Different types of quenching involved in photosystem II centers, *Biochim. Biophys. Acta 305*, 202−216.
49. Nugent, J. H., Muhiuddin, I. P., and Evans, M. C. (2002) Electron transfer from the water oxidizing complex at cryogenic temperatures: the S_1 to S_2 step, *Biochemistry 41*, 4117−4126.
50. Zhang, C., and Styring, S. (2003) Formation of split electron paramagnetic resonance signals in photosystem II suggests that $tyrosine_Z$ can be photooxidized at 5 K in the S_0 and S_1 states of the oxygen-evolving complex, *Biochemistry 42*, 8066−8076.
51. Koulougliotis, D., Teutloff, C., Sanakis, Y., Lubitz, W., and Petrouleas, V. (2004) The S_1Y_Z metalloradical intermediate in photosystem II: an X- and W-band EPR study, *Phys. Chem. Chem. Phys. 6*, 4859−4863.
52. Ioannidis, N., Zahariou, G., and Petrouleas, V. (2006) Trapping of the S_2 to S_3 state intermediate of the oxygen-evolving complex of photosystem II, *Biochemistry 45*, 6252−6259.
53. Ioannidis, N., and Petrouleas, V. (2000) Electron paramagnetic resonance signals from the S_3 state of the oxygen-evolving complex. A broadened radical signal induced by low-temperature near-infrared light illumination, *Biochemistry 39*, 5246−5254.
54. Zhang, C., Boussac, A., and Rutherford, A. W. (2004) Low-temperature electron transfer in photosystem II: a tyrosyl radical and semiquinone charge pair, *Biochemistry 43*, 13787−13795.
55. Havelius, K. G. V., Su, J. H., Feyziyev, Y., Mamedov, F., and Styring, S. (2006) Spectral resolution of the split EPR signals induced by illumination at 5 K from the S_1, S_3, and S_0 states in photosystem II, *Biochemistry 45*, 9279−9290.
56. Koulougliotis, D., Shen, J. R., Ioannidis, N., and Petrouleas, V. (2003) Near-IR irradiation of the S_2 state of the water oxidizing complex of photosystem II at liquid helium temperatures produces the metalloradical intermediate attributed to S_1Y_Z*, *Biochemistry 42*, 3045−3053.
57. Renger, G. (2004) Coupling of electron and proton transfer in oxidative water cleavage in photosynthesis, *Biochim. Biophys. Acta 1655*, 195−204.
58. Berthold, D. A., Babcock, G. T., and Yocum, C. F. (1981) A highly resolved, oxygen-evolving photosystem II preparation from spinach thylakoid membranes, *FEBS Lett. 134*, 231−234.
59. Völker, M., Ono, T., Inoue, Y., and Renger, G. (1985) Effect of trypsin on PS II particles: Correlation between Hill-activity, Mn-abundance and peptide pattern, *Biochim. Biophys. Acta 806*, 25−34.
60. Arnon, D. I. (1949) Copper enzymes in isolated chloroplasts. Polyphenoloxidase in *Beta vulgaris*, *Plant Physiol. 24*, 1−15.
61. Feyziyev, Y., van Rotterdam, B. J., Bernat, G., and Styring, S. (2003) Electron transfer from cytochrome b_{559} and $tyrosine_D$ to the S_2 and S_3 states of the water oxidizing complex in photosystem II, *Chem. Phys. 294*, 415−431.
62. Geijer, P., Deak, Z., and Styring, S. (2000) Proton equilibria in the manganese cluster of photosystem II control the intensities of the S_0 and S_2 state $g \sim 2$ electron paramagnetic resonance signals, *Biochemistry 39*, 6763−6772.
63. Roncel, M., Ortega, J. M., and Losada, M. (2001) Factors determining the special redox properties of photosynthetic cytochrome b559, *Eur. J. Biochem. 268*, 4961−4968.
64. Zhang, C. (2006) Interaction between $tyrosine_Z$ and substrate water in active photosystem II, *Biochim. Biophys. Acta 1757*, 781−786.
65. Boussac, A., and Etienne, A. L. (1982) Oxido-reduction kinetics of Signal II slow in tris-washed chloroplasts, *Biochem. Biophys. Res. Commun. 109*, 1200−1205.
66. Vass, I., and Styring, S. (1991) pH-dependent charge equilibria between tyrosine-D and the S states in photosystem II. Estimation of relative midpoint redox potentials, *Biochemistry 30*, 830−839.
67. Ishikita, H., and Knapp, E. W. (2006) Function of redox-active tyrosine in photosystem II, *Biophys. J. 90*, 3886−3896.
68. Meyer, B., Schlodder, E., Dekker, J. P., and Witt, H. T. (1989) O_2 evolution and Chl-a_{II}^+ ($P\text{-}680^+$) nanosecond reduction kinetics in single flashes as a function of pH, *Biochim. Biophys. Acta 974*, 36−43.
69. Haumann, M., Mulkidjanian, A., and Junge, W. (1999) Tyrosine-Z in oxygen-evolving photosystem II: a hydrogen-bonded tyrosinate, *Biochemistry 38*, 1258−1267.
70. Geijer, P., Morvaridi, F., and Styring, S. (2001) The S_3 state of the oxygen-evolving complex in photosystem II is converted to the S_2Y_Z* state at alkaline pH, *Biochemistry 40*, 10881−10891.
71. Hays, A. M. A., Vassiliev, I. R., Golbeck, J. H., and Debus, R. J. (1999) Role of D1-His190 in the proton-coupled oxidation of tyrosine Y_Z in manganese-depleted photosystem II, *Biochemistry 38*, 11851−11865.
72. Kühn, P., Pieper, J., Kaminskaya, O., Eckert, H. J., Lechner, R. E., Shuvalov, V., and Renger, G. (2005) Reaction pattern of photosystem II: oxidative water cleavage and protein flexibility, *Photosynth. Res. 84*, 317−323.
73. Rutherford, A. W., Boussac, A., and Faller, P. (2004) The stable tyrosyl radical in photosystem II: why D?, *Biochim. Biophys. Acta 1655*, 222−230.
74. Diner, B. A., Bautista, J. A., Nixon, P. J., Berthomieu, C., Hienerwadel, R., Britt, R. D., Vermaas, W., and Chisholm, D. A. (2004) Coordination of proton and electron transfer from the redox-active tyrosine, Y_Z, of photosystem II and examination of the electrostatic influence of oxidized tyrosine, $Y_D^{\bullet}(H^+)$, *Phys. Chem. Chem. Phys. 6*, 4844−4850.
75. Sugiura, M., Rappaport, F., Brettel, K., Noguchi, T., Rutherford, A. W., and Boussac, A. (2004) Site-directed mutagenesis of *Thermosynechococcus elongatus* photosystem II: the O_2-evolving enzyme lacking the redox-active tyrosine D, *Biochemistry 43*, 13549−13563.

BI700377G